Ninth International Conference on CFD in the Minerals and Process Industries
CSIRO, Melbourne, Australia
10-12 December 2012

EFFECT OF BUOYANCY ON METHANE GAS DISTRIBUTION AND GAS CONTROL STRATEGIES AT TAILGATE REGION IN A GASSY COAL MINE

Krishna TANGUTURI*, Rao BALUSU, Ramakrishna MORLA, Manoj KHANAL

CSIRO, Centre for Earth Science and Resource Engineering(CESRE), Queensland Centre for Advanced Technologies (QCAT), PO Box 4069, Kenmore, Australia

*Corresponding author Email: Krishna.Tanguturi@csiro.au

ABSTRACT

Methane (CH_4) gas emission is high in the goaf for a gassy coal mine and diffusion of the gas into the face will lead to hazardous working environment which can create operational difficulties. Electrical equipment which are loaded with sensors get tripped off when CH_4 level is greater than 2%. Diffusion of goaf gas into the face mainly depends upon the goaf orientation and the ingress of oxygen into the goaf. Goaf orientation will vary the buoyancy effects and affects the gas distribution. Oxygen ingresses more on the maingate (MG) side of the goaf due to a high ventilation air pressure and hence no major gas issues are dealt on this side of the goaf. However when the air flows along the face, air pressure decreases and less oxygen ingresses in the goaf on the tailgate (TG) side which leads to diffusion of CH_4 gas into the face. It not only disrupts the functioning of electrical equipment but also creates hazardous environment for the operator. In this paper, an attempt is made to understand the CH_4 gas distribution when the goaf orientation is at downdip angles of 2^o, 4^o and 6^o with respect to horizontal and investigate the gas control options like goaf drainage and back return systems to minimise the CH_4 level in the TG region. From the Computational Fluid Dynamics (CFD) investigations, it was concluded that for all downdip angle orientations the CH_4 concentration level at the TG region is above 2% and demand for control measures. Gas control strategy with goaf drainage was able to reduce the CH_4 level to below 1% and back return system at the TG side was able to completely eliminate CH_4 traces.

NOMENCLATURE

$\vec{V}$	Velocity Vector
$\vec{f}$	Body force vector per unit mass
$\vec{S}$	Source Vector per unit mass
p	Static Pressure
Y	Mass fraction of the species
u_i	Velocity along i /x direction
D_m	Coefficient of mass diffusivity
D_{ij}	Viscous Resistance Coefficient
C_{ij}	Inertia Resistance Coefficient in Porous matrix
μ	Coefficient of molecular viscosity
ρ	Mass density
$\dot{\omega}$	Rate of generation of mass per unit mass
τ	Stress Tensor
δij	Kronecker delta
ε	Specific dissipation rate
κ	Turbulent kinetic energy
μ_T	Eddy Viscosity

INTRODUCTION

Goaf gas emission has increased substantially over the years and is set to increase in the near future due to a high production rates, deeper mines and industry's trend towards wider and longer panels. High CH_4 emission from the goaf is one of the major issues which leads to spontaneous combustion in underground coal mines. In general, goaf gas emissions in number of gassy mines are of the order of 1000 to 4000 l/s. Aziz et al (1993), Baafi et al (1993) and Claassen (2011) used numerical techniques to understand the ventilation mechanisms, gas and dust distributions in coal mines. Balusu et al (2001,2002,2005) intensively carried out numerical investigations for understanding goaf gas distribution in gassy mines and invented various inertization strategies for prevention of spontaneous combustion in those mines. Most of the numerical studies carried out earlier provided an understanding on the overall oxygen and CH_4 distributions in gassy mines, however none of them were focused to investigate the gas distributions at TG region of the face. It is essential to understand the CH_4 gas distribution at the TG region for different downdip orientation of the goaf. Such details will assist in developing gas control strategies for safe operation of the coal mine. CH_4 diffusion into the face depends upon the goaf orientation. At the TG region high concentration of CH_4 are observed due to a less ingress of oxygen into the goaf. When CH_4 concentration is greater than 2%, the sensor trips off the electrical equipment and hampers all the mining operations. In these situations, ventilation air alone is not sufficient to control CH_4 gas levels and it is necessary to use other gas control strategies for reducing or eliminating CH_4 traces. The main objectives of this paper were to understand the goaf gas behaviour and its distribution near the TG region and to develop goaf gas control strategies and demonstrate their effectiveness. Initially, CFD investigations were carried out to determine the CH_4 level near the TG region for various downdip orientations of the goaf. Later, gas management strategies like goaf drainage and back return systems were used to control CH_4 concentration level.

Item/Descriptions	Full-Scale
Length of the goaf	1100 m
Width of the goaf	300 m
Goaf height above caving	80 m
Coal seam thickness	3.6 m
Top coal caving height	3.4m

Floor height below the face	12 m
Height of the main/tail gate roadway	3.6m
Width of the main/tail gate roadway	5.6 m

Table 1: CFD Model geometry dimensions

GEOMETRY

All the dimensions of the CFD model are specified in table 1. In figure 1 (a), the length of the goaf is 1100m, width is 300m and in figure 1 (b), the face retreat is 4^o downdip with MG down and TG up and the goaf is in 2^o inclination with respect to the horizontal. In figure 1(c) height of the goaf is 80m above the floor. The floor height is 12m below the face.

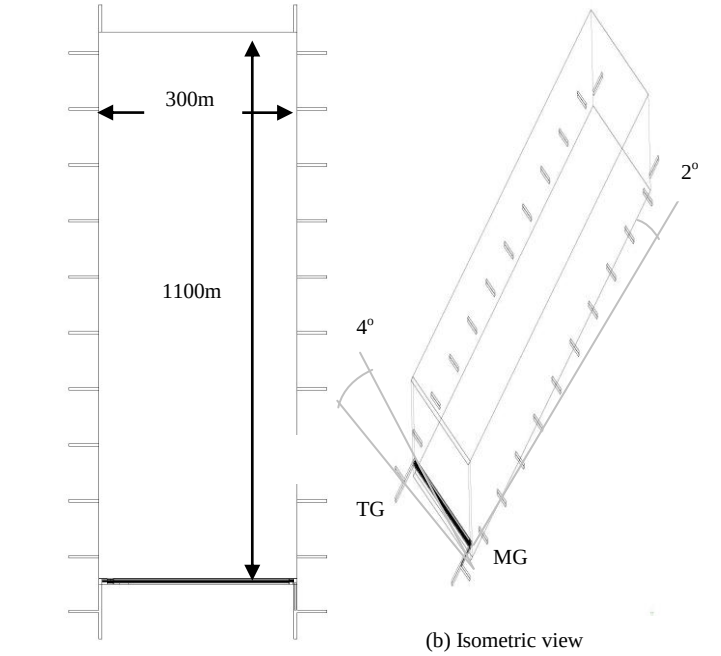

(a) Top View

(b) Isometric view

(c) Side view

Figure 1: Schematic diagram of the geometry

MODELLING AND MESHING

The model was created in ANSYS design modeller and was meshed with the default ANSYS (2012) mesh tool. Due to the geometrical complexities, prism type elements were used in the face and hexahedral elements were used in the goaf, as shown in figure 2. For reducing the computational effort, the total number of control volume used for meshing the geometry was limited to approximately 800,000 and based on the property gradients, the control volumes were denser in the face where air flows. The dimensions of the cells in the face varied between 0.2cm to 0.4cm and the length of the cell varied between 0.5m to 2m along the face. The cell dimensions in the goaf region were very large and varied between 1m near the face to 10m in the mid and end of the goaf region. The simulated results give firsthand information regarding the gas control approaches. The mesh in the goaf is 10m and any further reduction poses a limitation on computational effort.

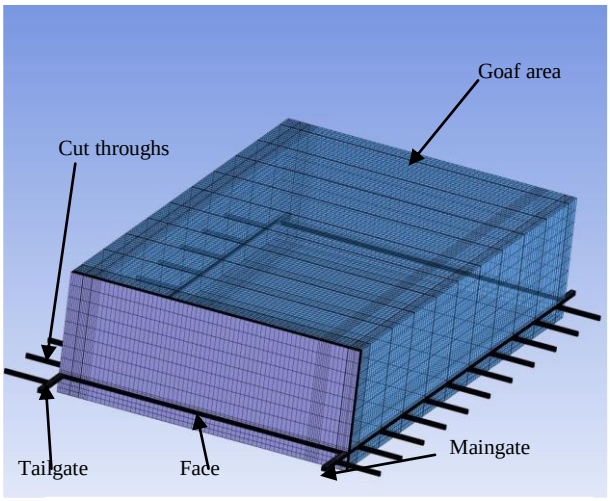

Figure 2: Meshed geometry

MATHEMATICAL MODEL

The instantaneous conservative equations i.e., continuity, Navier Stokes and the species transport equations were solved numerically using finite volume discretisation techniques. These equations were solved in the goaf region where the flow was laminar. Note that the goaf region was treated as porous media with resistances varying in all the three directions. The time averaged governing equations were solved in the face region where the flow was turbulent

Continuity equation for incompressible air flow

$$\nabla \bullet \vec{V} = 0.0 \tag{1}$$

Steady State Navier Stokes Equation for incompressible flow

$$(\vec{V} \bullet \nabla)\rho\vec{V} = -\nabla p + \mu\nabla^2\vec{V} + \rho\vec{f} + \vec{S} \tag{2}$$

Steady State Species Transport Equation

$$(\vec{V_s} \bullet \nabla)\rho Y_s = D_{ms}\nabla^2 Y + \dot{\omega}_s \tag{3}$$

where subscript s represents properties of O_2, CH_4 and N_2.

Turbulence Modelling

The flow was assumed to be turbulent in the face region and the time averaged equations were solved. Two equation standard k-epsilon model was used to determine the eddy viscosity and the Reynolds stresses in the flow. It has to be noted here that the instantaneous equations are solved in the goaf region where the flow is treated as laminar. The time averaged equations are solved only in the face region where the flow is turbulent.

Time Averaged Governing Equations

Continuity Equation:

$$\nabla \bullet \vec{V} = 0.0 \tag{4}$$

Reynolds Averaged Navier Stokes Equation:

$$(\vec{V} \bullet \nabla)\rho\vec{V} = -\nabla\overline{P} + \mu\nabla^2\vec{V} + \nabla : \tau_R \tag{5}$$

where τ_R is the Reynolds stress tensor.

Turbulent Kinetic Energy- k equation:

$$\rho\overline{u_j}\frac{\partial k}{\partial x_j} = \tau_{ij}\frac{\partial\overline{u_i}}{\partial x_j} + \frac{\partial}{\partial x_j}\left((\mu + \frac{\mu_T}{\sigma_k})\frac{\partial k}{\partial x_j}\right) - \rho\varepsilon \tag{6}$$

where subscript j represents Einstein summation notation.

Turbulent dissipation- ε equation:

$$\rho\overline{u_j}\frac{\partial \varepsilon}{\partial x_j} = C_{\mu 1}\tau_{ij}\frac{\partial\overline{u_i}}{\partial x_j} + \frac{\partial}{\partial x_j}\left((\mu + \frac{\mu_T}{\sigma_\varepsilon})\frac{\partial \varepsilon}{\partial x_j}\right) - C_{\mu 2}\rho\frac{\varepsilon}{k^2} \tag{7}$$

where Cμ1 and Cμ2 are closure coefficient.

Reynolds Stress:

$$\tau_{ij} = \mu_T\left(\frac{\partial\overline{u_i}}{\partial x_j} + \frac{\partial\overline{u_j}}{\partial x_i}\right) - \frac{2}{3}\rho k\delta_{ij} \tag{8}$$

where μ_T is the eddy viscosity and δ_{ij} is Kronecker delta.

Eddy Viscosity:

$$\mu_T = c_\mu\rho\frac{k^2}{\varepsilon} \tag{9}$$

where c_μ is closure coefficient which is equal to 0.07.

Porous media model

Front leg, lemniscate linkage and the canopy region of the geometry were modelled as porous zones. The porous media model was used to simulate the flow though the porous regions by the addition of a momentum source term to the standard fluid flow equations. The source term is composed of two parts: a viscous loss term (Darcy law), and an inertial loss term.

$$\vec{S} = -\left(\sum_{j=1}^{3} D_{ij}\mu\vec{V} + \sum_{j=1}^{3} C_{ij}\frac{1}{2}\rho\left|\vec{V}\right|\vec{V}\right) \tag{10}$$

Source term in the momentum equation contributes to the pressure gradient in the porous cell, which is proportional to the fluid velocity in the cell. Further information regarding the model can be obtained in ANSYS FLUENT manual (2012). In the CFD model, the incorporation of goaf spatial permeability distribution and gas emission were inputted via a user defined function (UDF) that was linked to the ANSYS-FLUENT solver.

BOUNDARY CONDITIONS AND SOURCE TERMS

At MG, an inlet velocity corresponding to 60m^3/s flow rate was specified and at the TG exit an outflow boundary condition was specified. The buoyancy effects were incorporated in the model via components of gravity along x and z directions. In the goaf, CH_4 gas emission rate of 1000l/s was specified via the UDF as the source term to the species transport equation. CH_4 emission in the goaf is a function of space and no emissions exists in the face region.

NUMERICAL SIMULATION

First order schemes were used to discretize the governing equations as the cell size was very large and second order schemes failed to converge. Coupling between the pressure term and velocity was done using SIMPLE algorithm. Flow was assumed to be laminar in the goaf region and instantaneous equations were solved in this region, and flow was assumed to be turbulent in the face region and all the time averaged steady state equations were solved here. Standard κ-ε model was used to calculate additional stresses induced in the flow due to turbulence. All the governing equations were solved until the convergence criteria of order 10^{-4} was reached.

RESULTS

Figures 3 and 4 indicate measured and simulated velocities across the face at the mid face and 5m from the TG corner. Figure 3 (a) indicated the spot velocities at various locations across the face at the mid face. The velocities were measured using an anemometer. In figure 3 (b), at the mid of the face, the flow is fully developed and high velocities were observed near the face region and the velocity magnitude reduces across the face till the back of the face. Due to the resistance in the leg, lemniscate linkage and in the canopy regions, which are treated as porous regions, the velocities were low. Figure 4 (a) indicates the spot velocities at various locations across the face at 5m from the TG exit. In figure 4 (b) at 5m from the TG exit, the velocities at the rear of the face were very less. Simulated velocities match with the measured sample points across the face with a minor error. The low velocities and pressure across the back of the face region led to a less ingress of oxygen into the goaf which further led to more diffusion of the CH_4 gas into the face region especially near the TG corner. In figure 5, the oxygen distribution is shown for various face downdip angles. It was observed that for all the downdip angle orientations, oxygen ingress deep into the goaf on the MG side and less on the TG side. In figure 5 (a), for a downdip angle of 2^o low oxygen level was seen at the centre of the goaf. In figure 5 (b) and (c), as the down dip angle was increased to 4^o and 6^o oxygen ingresses into the centre and top of the goaf.

In figure 6 (a) the CH_4 distribution is seen to be high at the centre of the goaf for a 2^o downdip angle and as the downdip angle increased from 2^o to 4^o and 6^o, as shown in figure 6 (b) and (c), CH_4 was pushed to the left and top of the goaf. Figure 7 is the enlarged view of the CH_4 levels at the TG corner. At 2^o downdip angle, figure 7 (a), high level of CH_4 was observed up to 50m on the TG side of the goaf. But when the downdip angle was increased to 4^o and 6^o, figure 7 (b) and 7 (c), the CH_4 fringes were pushed to the right side of the goaf and less CH_4 level was observed in the goaf. But in all the cases the CH_4 level at the TG corner was above 2% which violated the statutory limits for safe operation of the coal mine. To control the CH_4 concentration at the TG corner, goaf drainage and back return systems were used for CFD simulations.

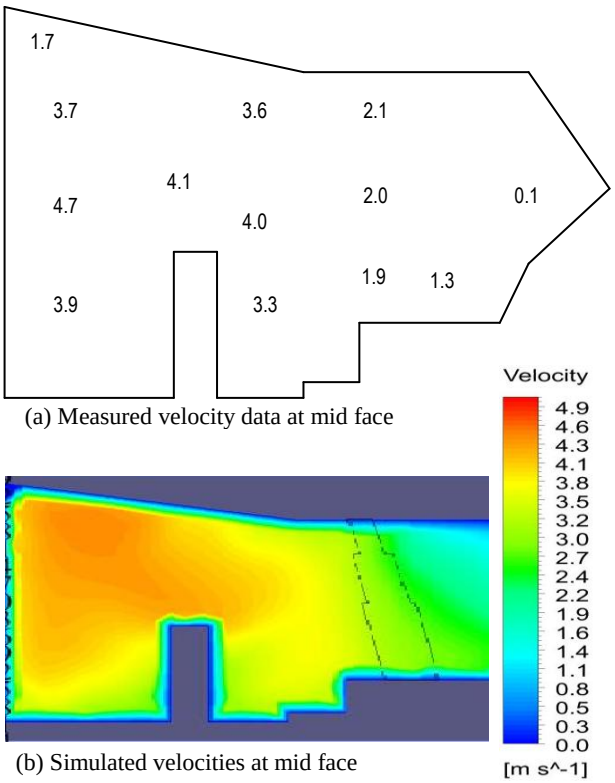

(a) Measured velocity data at mid face

(b) Simulated velocities at mid face

Figure 3: Measured and simulated velocities at mid face

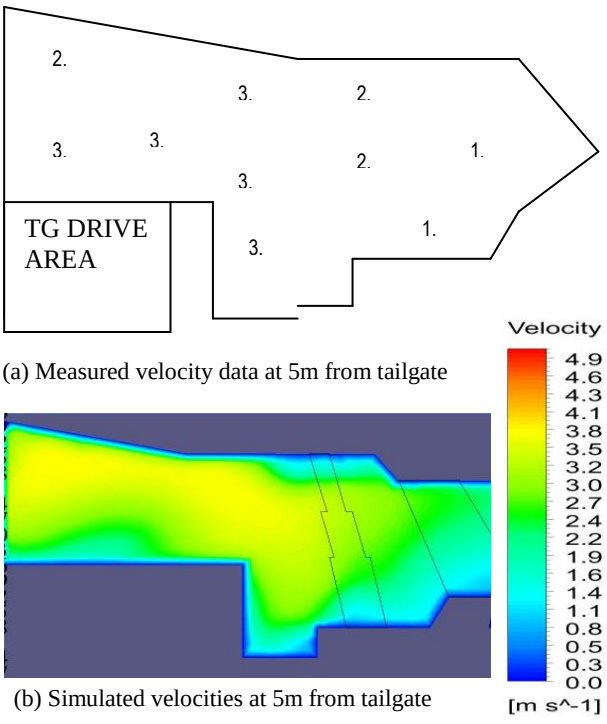

(a) Measured velocity data at 5m from tailgate

(b) Simulated velocities at 5m from tailgate

Figure 4: Measured and Simulated velocities at 5m from tailgate

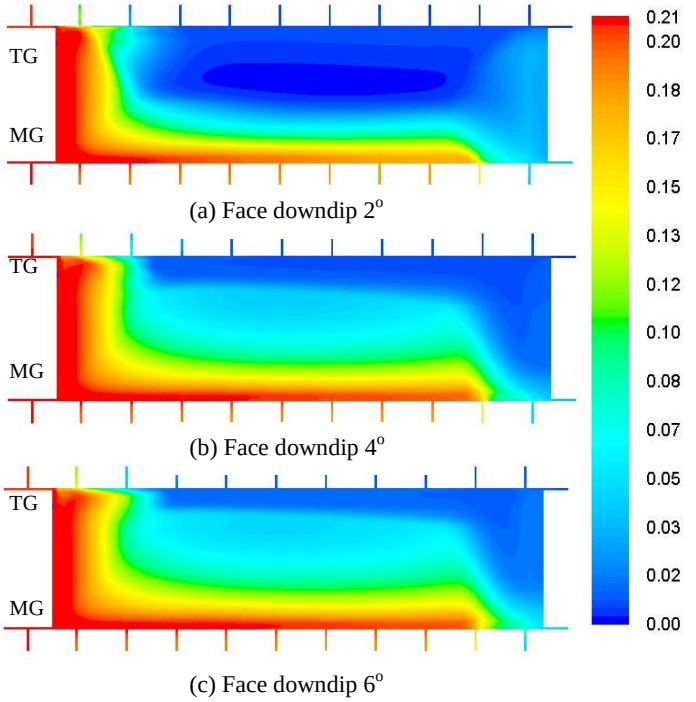

(a) Face downdip 2°

(b) Face downdip 4°

(c) Face downdip 6°

Figure 5: Oxygen distributions in the goaf on the plane containing the face

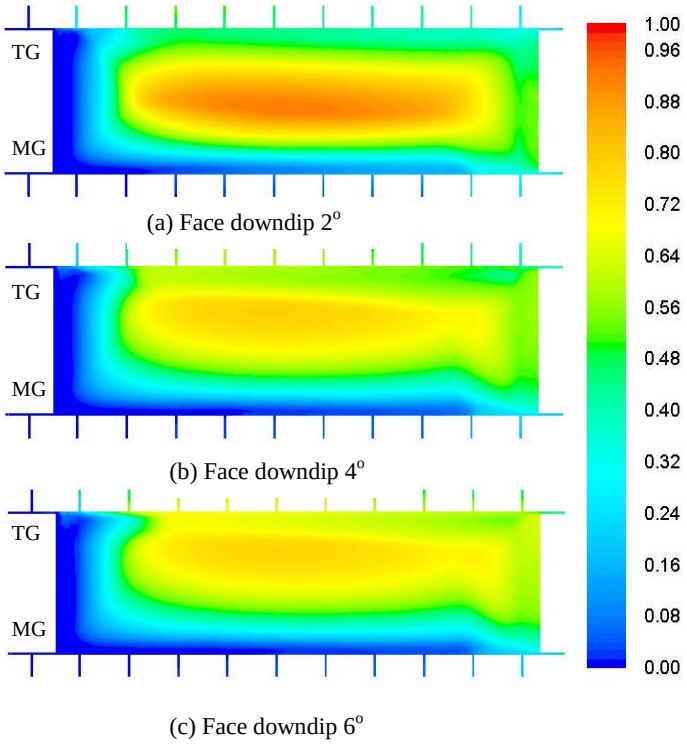

(a) Face downdip 2°

(b) Face downdip 4°

(c) Face downdip 6°

Figure 6: CH4 distributions in the goaf on the plane containing the face

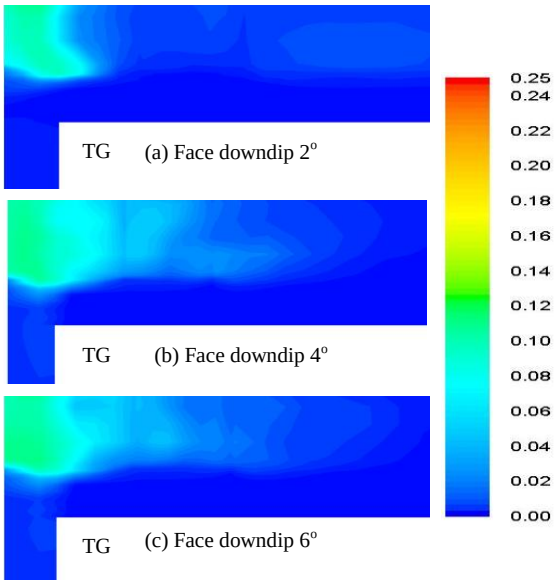

Figure 7: CH4 distributions in the goaf near TG region

GOAF GAS CONTROL STRATEGIES

CH_4 concentration near the TG region can be reduced by forcing oxygen ingress into the TG side of the goaf. This will assist in preventing methane gas diffusion in the TG region. Gas management strategies such as goaf gas drainage system and back returning system were also investigated to see their effects on CH_4 concentration near TG region.

Goaf Drainage System

Goaf holes were drilled at various locations for removing some of the CH_4 gas from the goaf. The location of the goaf hole is important for controlling the gas levels at the TG region. For simplicity CH_4 gas was removed from the second cut through on the TG side as shown in figure 8. Figure 9 indicates the methane concentration distribution in the goaf for gas drainage volume flow rates of 200, 400 and 600l/s near the TG region. Less CH_4 concentration was observed due to goaf gas drainage at the TG corner. As the drainage volume increased, figures 9 (a) (b) and (c), the concentration of CH_4 at the TG corner decreased and more gas was squeezed from the top of the goaf. The high concentration of CH_4 was also observed at the centre of the goaf.

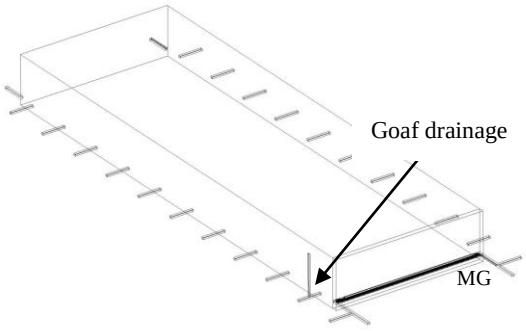

Figure 8: Goaf drainage through 2nd cut through on the tailgate side of the goaf

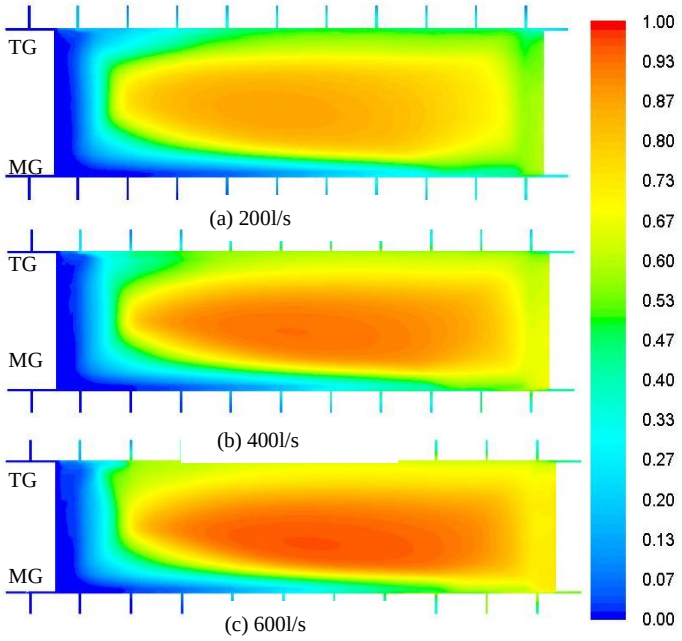

Figure 9: CH_4 distributions with goaf drainages

Figure 10 indicates the enlarged view of CH_4 gas distribution at the TG region for various volumes of goaf drainage. In all the cases the CH_4 levels near the TG region was less than 1%, which is within the statutory limits for safe operation of coal mine.

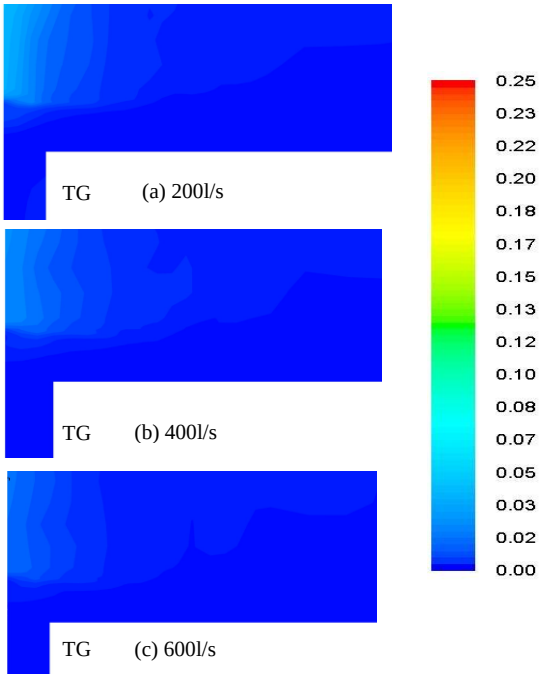

Figure 10: CH4 distributions near the TG region for various goaf drainage volumes

Back Return System

In a back return system, a part of the ventilated air is allowed to pass through the cut throughs on the TG side. In this case 15% of the ventilated air was used as the back returning air. The purpose of back returning the air was to increase the oxygen ingress in the goaf region on the TG side.

Figure 11 indicates a model with a back return system on the TG side from the 2nd cut through. In figure 12, due to the back return system, high concentration of oxygen can be seen in the TG region and at the mid of the goaf. Figure 13 shows an enlarged view of the TG corner which indicates a complete elimination of methane fringes i.e. methane shifted into the goaf region due to more oxygen ingress into the goaf on the TG side.

.

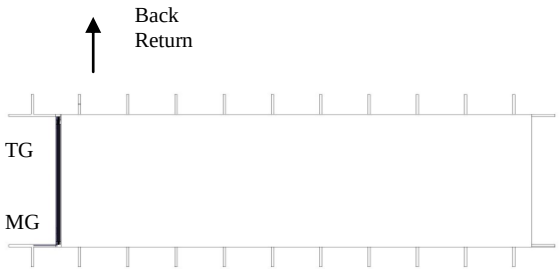

Figure 11: Back returning the ventilation quantity through the 2nd cut through

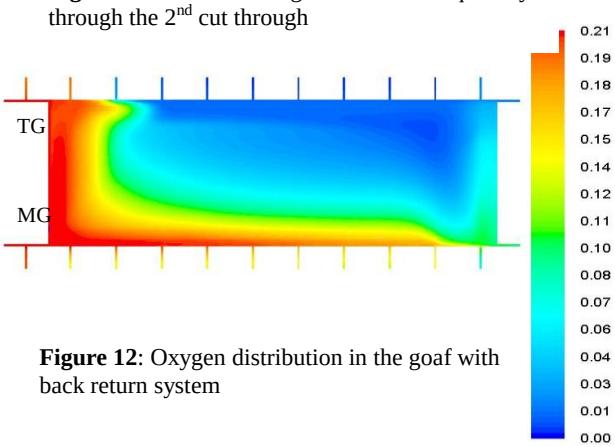

Figure 12: Oxygen distribution in the goaf with back return system

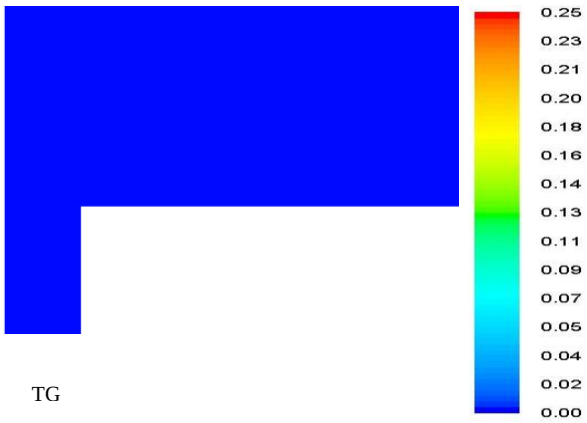

Figure 13: CH_4 distribution at the TG corner with back return system

CONCLUSIONS

It was concluded from the numerical simulations that the gas related issues exists on the TG side for various downdip orientation angles. Gas management strategies were recommended for preventing CH_4 gas diffusion near the TG motor regions. Gas management strategies like goaf drainage and back return systems were helpful in reducing the CH_4 gas concentration level to below 1%. In this study, goaf gas drainage of 200,400 and 600l/s reduced the CH_4 gas concentration to below 1%. It was also showed from the numerical simulation that the complete elimination of the methane gas traces was possible by back returning a part of the ventilated air quantity through the TG cut throughs.

REFERENCE

AZIZ, N, SRINIVASA, R.B. and BAAFI, E.(1993), Application of Computational Fluid Dynamics Codes to Develop Effective Gas/Dust Control Measures in Underground Coal Mines, *The Australian Coal Journal*, No42, p19-27.

BALUSU, R, DEGUCHI, G, HOLLAND, R, MOREBY, R, XUE S, WENDTL M and MALLET, C, (2001). Goaf gas flow mechanics and development of gas and sponcom control strategies at a highly gassy coal mine, *Australia-Japan Technology Exchange Workshop*, 3-4 December, Hunter Valley, Australia, 18 pp.

BALUSU R., PATRICK HUMPHRIES, PAUL HARRINGTON, MICHEAL WENDTL and SHENG XUE(2002), Optimum Inertisation Strategies, *Proceedings of the Queensland Mining Industry Health & Safety Conference*, 4 - 7 August, Townsville, Australia, pp 133 - 144.

PATANKAR V.SUHAS.(1980), "*Numerical Heat Transfer and Fluid Flow*, Washington, DC, Hemisphere Publishing Corp.

ANSYS FLUENT 14.0 reference manual 2012.

RAO BALUSU, R REN TX and HUMPHRIES P (2005) Proactive inertisation strategies and technologies development. *ACARP report* C 12020.

BAAFI, E.Y., AZIZ, N.I. and SRINIVASARAO.B(1993), 3-D finite element analysis and Pollutant behaviour in a Longwall Face, *Proceedings of 24th International symposium on Application of Computers and operations Research in the Mineral Industry*, Canada, pp 311-318.

C.CLAASSEN (2011) , Goaf Inertisation and sealing Utilising Methane from In-Seam Gas Drainage system, *11th Underground Coal Operators' conference*, University of Wollongong, pp 369-374.

BALUSU R, R, XUE S, WENDT M, MALLETT C, ROBERTSON B, HOLLAND R, MOREBY R, MCLEACND AND DEGUCHI(2002), An investigation of the gas flow mechanics in longwall goafs, *Proceedings of the North American / Ninth US Mine Ventilation Symposium*, Kingston, Ontario, Canada pp. 443-450.